ORIGINAL RESEARCH

In vivo alpha-V beta-3 integrin expression in human aortic atherosclerosis

William S Jenkins [ID],[1] Alex T Vesey,[1] Anna Vickers,[1] Anoushka Neale,[1] Catriona Moles,[1] Martin Connell,[2] Nikhil Vilas Joshi,[1] Christophe Lucatelli,[2] Alison M Fletcher,[2] James C Spratt,[1] Saeed Mirsadraee,[2] Edwin JR van Beek,[2] James HF Rudd [ID],[3] David E Newby,[1] Marc R Dweck[1]

ABSTRACT

Objectives Intraplaque angiogenesis and inflammation are key promoters of atherosclerosis and are mediated by the alpha-V beta-3 ($\alpha_v\beta_3$) integrin pathway. We investigated the applicability of the $\alpha_v\beta_3$-integrin receptor-selective positron emission tomography (PET) radiotracer 18F-fluciclatide in assessing human aortic atherosclerosis.

Methods Vascular 18F-fluciclatide binding was evaluated using ex vivo analysis of carotid endarterectomy samples with autoradiography and immunohistochemistry, and in vivo kinetic modelling following radiotracer administration. Forty-six subjects with a spectrum of atherosclerotic disease categorised as stable (n=27) or unstable (n=19; recent myocardial infarction) underwent PET and CT imaging of the thorax after administration of 229 (IQR 217–237) MBq 18F-fluciclatide. Thoracic aortic 18F-fluciclatide uptake was quantified on fused PET-CT images and corrected for blood-pool activity using the maximum tissue-to-background ratio (TBR_{max}). Aortic atherosclerotic burden was quantified by CT wall thickness, plaque volume and calcium scoring.

Results 18F-Fluciclatide uptake co-localised with regions of increased $\alpha_v\beta_3$ integrin expression, and markers of inflammation and angiogenesis. 18F-Fluciclatide vascular uptake was confirmed in vivo using kinetic modelling, and on static imaging correlated with measures of aortic atherosclerotic burden: wall thickness (r=0.57, p=0.001), total plaque volume (r=0.56, p=0.001) and aortic CT calcium score (r=0.37, p=0.01). Patients with recent myocardial infarction had greater aortic 18F-fluciclatide uptake than those with stable disease (TBR_{max} 1.29 vs 1.21, p=0.02).

Conclusions In vivo expression of $\alpha_v\beta_3$ integrin in human aortic atheroma is associated with plaque burden and is increased in patients with recent myocardial infarction. Quantification of $\alpha_v\beta_3$ integrin expression with 18F-fluciclatide PET has potential to assess plaque vulnerability and disease activity in atherosclerosis.

Check for updates

INTRODUCTION

Atherosclerotic cardiovascular disease is the most common cause of death worldwide, and elucidating the mechanisms underlying the propagation and rupture of atherosclerotic plaques remains a key public health goal.[1] Although our understanding of the pathogenesis underlying atherosclerosis has progressed over the last two decades, accurate prediction of clinical events remains elusive. There is therefore considerable interest in non-invasive imaging techniques that go beyond the detection of luminal stenoses and instead focus on measuring disease activity within the vasculature.[2 3]

Combined positron emission tomography (PET) and CT is a non-invasive hybrid imaging technique that integrates targeted functional molecular imaging with high-detail anatomical definition. This technique has been used to quantify vascular inflammation and calcification activity with success in both carotid and coronary atherosclerosis.[4–7] Recently, intraplaque angiogenesis and neovascularisation has emerged as a key factor in the development, progression and instability of atherosclerotic plaques.[8] The integrin alpha-V beta-3 ($\alpha_v\beta_3$) cell surface receptor is upregulated on endothelial cells in states of angiogenesis and is also observed on macrophages at sites of increased vascular inflammation, another key contributor to plaque instability. This receptor helps coordinate interaction between cellular components and the extracellular matrix, and contains a distinctive RGD-amino acid sequence (the arginine-glycine-aspartate motif) in the cell-ligand interaction site. On this basis, several PET tracers targeting the RGD sequence have been developed for monitoring angiogenesis in malignant tumours.[9 10] These tracers have also shown promise in monitoring atherosclerotic activity in preclinical models[8 11–14] and in a recent small study of patients with carotid atheroma.[7]

18F-Fluciclatide is a novel RGD-based PET radiotracer with high affinity for the $\alpha_v\beta_3$ integrin receptor.[10 15 16] We hypothesised that 18F-fluciclatide may act as an imaging marker of atherosclerotic disease activity in vivo, informing about both inflammation and angiogenesis. In this study, we sought to characterise the cellular and imaging characteristics of 18F-fluciclatide uptake in human atherosclerosis using a clinical cohort of patients with both stable and unstable clinical disease.

METHODS

Study populations

In total we studied 50 patients. Four patients were recruited who had sustained a recent stroke and were undergoing carotid endarterectomy. In these patients, excised carotid plaques were examined

using histology and 18F-fluciclatide autoradiography. For in vivo imaging, 46 patients were recruited from the Royal Infirmary of Edinburgh between July 2013 and December 2014. This cohort comprised 19 *unstable* patients with a recent acute ST-segment elevation myocardial infarction (MI) (14±7 days after MI) (NCT01813045),[17] and 27 *stable* patients with either stable angina (n=6) or asymptomatic atherosclerotic disease (n=21; 12 had calcific aortic valve disease) (NCT01837160). Exclusion criteria were age <40 years, women of childbearing potential, severe renal failure (estimated glomerular filtration rate <30 mL/min) or hepatic failure (Child-Pugh grade B or C), atrial fibrillation, known contrast allergy, inability to undergo scanning and inability to provide informed consent. All 46 subjects underwent 18F-fluciclatide PET imaging alongside clinical assessment that included evaluation of cardiovascular risk and high-sensitivity C-reactive protein (hs-CRP) measurement (Biocheck, Foster City, California, USA).

This study was conducted in accordance with the Declaration of Helsinki and with written informed consent of each participant.

Radiosynthesis of 18F-fluciclatide

18F-Fluciclatide was manufactured at the Clinical Research Imaging Centre on an automated module (FASTlab synthesiser; GE Healthcare) by coupling an amino-oxy-functionalised peptide precursor (AH111695) with 4–18F-fluorobenzaldehyde at pH 3.5 to form 18F-fluciclatide.[17] A full description of this synthesis has been published previously.[16]

Histological validation

Carotid endarterectomy specimens (online supplementary data) were fresh frozen and sectioned in cryosection medium. Both atheromatous and non-atheromatous segments were fixed, stained with H&E and examined by immunohistochemistry for smooth muscle actin, CD31, CD68 and $\alpha_v\beta_3$ integrin receptor expression before digital image capture (Axioscan.Z1, Zeiss, UK). Image analysis was performed on ImageJ32 software (National Institutes of Health, Bethesda, Maryland, USA). Staining was expressed as a percentage of the total plaque area and with an object size set threshold applied at 20×10 pixels, to limit counting to cell-sized objects. The density of cell staining in the endarterectomy tissue was expressed as cells per mm^2.[18]

Autoradiography was performed to identify the precise localisation of 18F-fluciclatide binding in atherosclerotic tissue. Carotid sections were bathed in a solution of 18F-fluciclatide (1 kBq/mL) for 60 min and rinsed with phosphate buffer solution. To rule out non-specific radiotracer uptake, an un-labelled highly concentrated solution of fluciclatide was added to bind competitively with the $\alpha_v\beta_3$ integrin receptors. 18F-Fluciclatide binding was imaged using a FujiFilm FLA-5100 Fluorescent Image Analyser (Raytek Scientific, Sheffield, UK).

Clinical 18F-fluciclatide PET imaging

All patients in the imaging cohort underwent PET-CT imaging of the thorax with a hybrid scanner (Biograph mCT, Siemens Medical Systems, Erlangen, Germany) at the Clinical Research Imaging Centre, University of Edinburgh. Subjects were administered a target dose of 230 MBq 18F-fluciclatide. An attenuation correction CT scan (non-enhanced 120 kV and 50 mA, 3 mm slices) was performed prior to PET acquisition. To define tracer pharmacodynamics and the optimum timing of scanning, dynamic PET imaging of the thorax was performed in the initial 20 patients in three-dimensional (3-D) mode using a single bed position for 70 min. For the remainder of the study subjects, static imaging was performed at the optimal time point (found to be 40 min postinjection) using a single 30 min bed position in list mode with electrocardiographic gating. Immediately after PET acquisition, thoracic CT angiography was performed (online supplementary data).

PET image reconstruction and analysis

Kinetic analysis was performed on the dynamic PET studies to investigate the pharmacodynamics of 18F-fluciclatide uptake within atheroma. The methodology is described in detail in the online supplementary data. In all patients, static electrocardiogram-gated PET images were reconstructed in diastole (40–70 min postinjection, 50%–75% of the R-R interval, Ultra-HD, 2 iterations, 21 subsets, zoom ×2, 200 pixels). Images were analysed by experienced observers blinded to the demographic data (WJ, AV) using an OsiriX workstation (OsiriX V.6.0 64-bit; OsiriX Imaging Software, Geneva, Switzerland). PET images were fused with the attenuation correction CT, and regions of interest drawn around the thoracic aorta on serial axial slices just beyond the discernible adventitial border. Aortic uptake was assessed in three regions: the ascending thoracic aorta (from the level of mid-right pulmonary artery up to the last slice where the aorta maintained its circular cross-sectional appearance), the descending thoracic aorta (the region extending from the tip of the diaphragm up to the last circular slice) and the aortic arch (the region of the aorta connecting the ascending and descending aorta). Within these regions, mean and maximum tracer activities were measured using standard uptake values (SUV; the decay corrected tissue concentration of the tracer divided by the injected dose per body weight, kBq/mL) and corrected for mean radiotracer blood pool activity to provide a mean of the TBR_{max} (mean TBR_{max}).[5 19 20] The blood pool radiotracer activity was quantified in the superior vena cava (SVC), measured in the axial plane on 4–5 sequential 5 mm axial slices above the level of the junction of the left innominate vein. In a substudy of 10 randomly selected subjects, images were assessed independently by two experienced observers and the interobserver reproducibility of 18F-fluciclatide SUV and TBR measurements assessed.

CT image reconstruction and analysis

The aortic CT calcium score was calculated for the aorta as a whole and for its different regions using axial slices on the attenuation correction CT dataset (OsiriX V.6.0 64-bit; OsiriX Imaging Software) and expressed in arbitrary units (AU).[21] In those patients whose descending aorta was visualised within contrast CT datasets (n=33), further measures of aortic atherosclerotic plaque burden were made on dedicated plaque analysis software (Vital Images, Minnetonka, Minnesota, USA). Using the sagittal plane, the entire portion of the descending thoracic aorta within the field of contrast CT acquisition was delineated and the luminal blood pool removed using semi-automated thresholding. The mean aortic wall thickness was recorded and corrected for the vessel diameter providing the indexed wall thickness. Additionally, the aortic wall volume was recorded and corrected for total vessel volume to provide an indexed plaque volume.

Statistical analysis

Continuous data were tested for normality visually and with the D'Agostino-Pearson omnibus test. Continuous data were presented as median (IQR) and compared using Pearson's or

Spearman's correlation or Wilcoxon signed-rank test as appropriate. Aortic calcium score and hs-CRP were log-transformed to base 10 to achieve normality prior to statistical analysis. Interobserver reproducibility was calculated by Bland Altman method and presented as mean bias ±2 SD, and intraclass correlation coefficients (ICC).[22] Mann-Whitney U test was used to assess continuous variables across groups of a categorical variable. A matched stable atheroma group was created through censoring of patients with stable atheroma and high levels of aortic calcification by researchers blinded to the PET data. Statistical analysis was performed with GraphPad Prism V.6 (GraphPad Software, California, USA). A two-sided $p < 0.05$ was taken as statistically significant.

RESULTS

Plaque autoradiography and histology

Autoradiography of carotid plaque demonstrated focal 18F-fluciclatide binding in regions of advanced atherosclerosis that was effectively blocked by un-labelled fluciclatide (figure 1A, B). On adjacent tissue sections processed for histology, these regions of ex vivo 18F-fluciclatide uptake co-localised with areas of intense cellular staining of $\alpha_v\beta_3$ integrin (45.2 (29.1–66.9) cells/mm^2, % area 4.2 (3.2–5.7)), microvascular endothelial cells at sites of angiogenesis and positive remodelling (CD31+; 23.0 (6.5–63.0) cells/mm^2, % area 2.5 (2.2–4.9)), and inflammatory macrophages deeper adjacent to the necrotic core (CD68+; 32.0 (21.0–49.8) cells/mm^2, % area 3.7 (2.4–5.6), figure 1C–H). By comparison regions of carotid endarterectomy specimen without visible atheroma did not demonstrate 18F-fluciclatide uptake, and had much lower levels of $\alpha_v\beta_3$ integrin receptor expression (4.5 (4.3–5.2) cells/mm^2, % area 0.6 (0.5–2.0), both $p = 0.05$ compared with areas with increased 18F-fluciclatide expression), as well as staining for both angiogenic endothelial cells (CD31+; 2.1 (1.8–2.4) cells/mm^2, % area 0.9 (0.6–1.2), both $p = 0.05$) and inflammatory macrophages (CD68+; 4.3 (2.8–4.4) cells/mm^2, % area 0.6 (0.5–1.2), both $p = 0.03$).

In vivo imaging cohort

A total of 46 subjects underwent PET imaging with CT angiography (age 66±10 years, 74% male; table 1) following injection of 229 (IQR 217–237) mBq 18F-fluciclatide. Of the 46 subjects recruited, 19 had suffered a recent MI (*unstable cohort*), and 27 had imaging evidence of aortic atherosclerosis on CT but no recent cardiovascular events (*stable cohort*: 6 with stable angina and 21 with subclinical disease who were asymptomatic with no prior cardiovascular events). Interestingly, those in the stable cohort had greater aortic calcification than patients in the unstable group (AU (IQR); 326 (11–1114) vs 19 (0–483), $p < 0.01$), reflecting their greater age (years (IQR); 69 (66–74) vs 60 (51–70), $p = 0.01$). The groups were well matched for gender ($p = 0.97$) and body mass index ($p = 0.39$), and were both characterised by high prevalence of atherosclerotic risk factors, with more smokers in the unstable group ($p < 0.001$) and more patients with hypertension in the stable group ($p = 0.02$). No adverse events were reported following administration of 18F-fluciclatide and the average total radiation dose per participant was 15 mSv.

Dynamic analysis of aortic 18F-fluciclatide uptake

On kinetic analysis (n=20), activity within aortic atheroma increased gradually, reaching a plateau at 40–70 min. Injected 18F-fluciclatide activity has a biexponential blood pool clearance with a half-life of about 10 min consisting of a fast redistribution
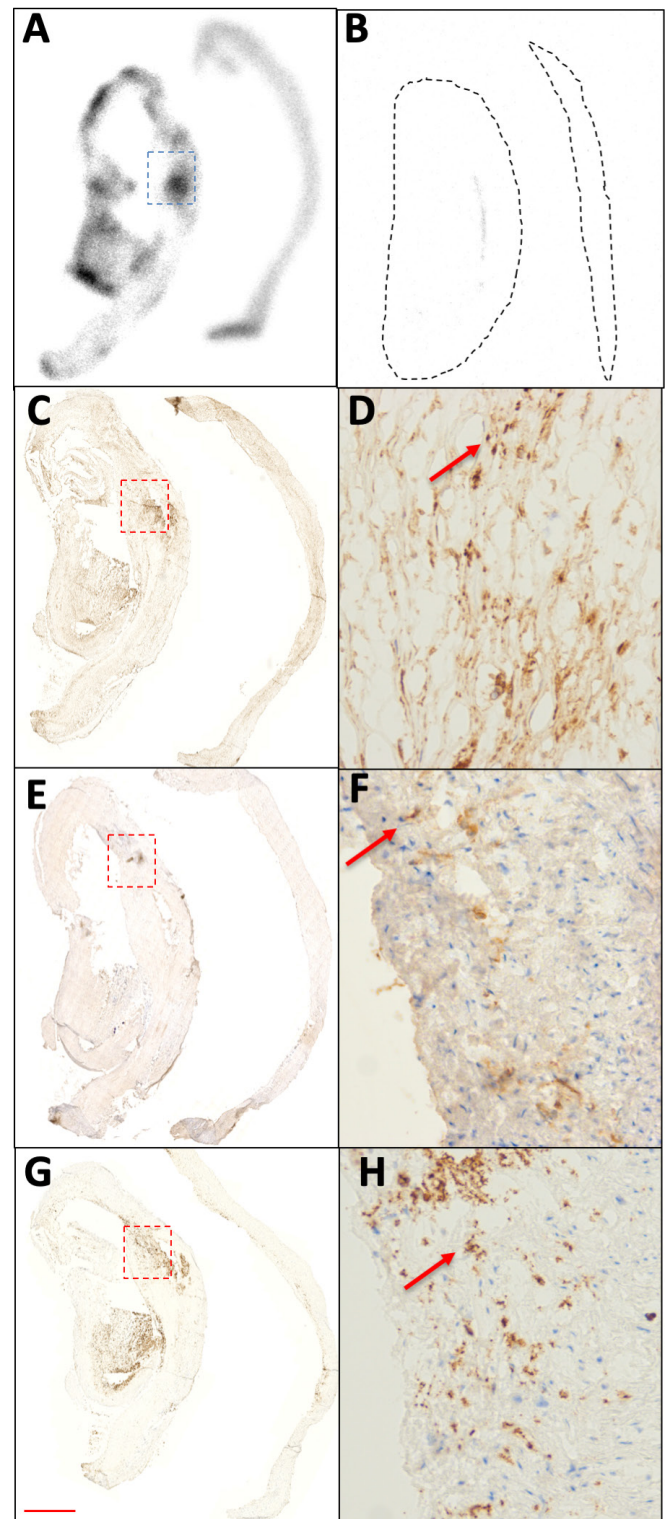
Figure 1 18F-Fluciclatide uptake in carotid atheroma. (A) Autoradiography image of segments of ruptured carotid plaque (left) and proximal healthy segments (right). Greater 18F-fluciclatide binding is visible within plaque rupture segments. Binding within the tissue segments (demarcated, black) was successfully blocked by the addition of a more concentrated un-labelled solution of fluciclatide (B). Areas showing the highest fluciclatide binding (demarcated, blue) exhibited a high degree of alpha-V beta-3 integrin expression (C and D, arrow) that also featured cellular staining for vascular endothelial cells (CD31, E and F, arrow) and inflammatory cells (CD68, G and H, arrow). Scale bar=1 mm in C, E, G and 75 µm in D, F, H.

Table 1 Patient characteristics

	All (n=46)	Stable atherosclerosis (n=27)	Unstable atherosclerosis (n=19)	P value*
Age (years)	67 (60–74)	69 (66–74)	60 (51–70)	0.01
Male sex	34 (74)	20 (74)	14 (74)	0.97
BMI (kg/m^2)	28 (25–31)	28 (24–30)	27 (25–32)	0.39
Systolic BP (mm Hg)	140 (124–160)	149 (134–167)	125 (114–139)	<0.001
18F-Fluciclatide dose (MBq)	229 (217–237)	228 (217–236)	229 (215–240)	0.69
Cardiovascular history				
Angiographically documented CAD	26 (57)	7 (26)	19 (100)	<0.001
Prev MI	24 (52)	5 (19)	19 (100)	<0.001
Prev PCI	20 (43)	2 (7)	18 (95)	<0.001
Prev CVD	4 (11)	4 (14)	0 (0)	0.08
Risk factors				
Current smoker	9 (20)	1 (4)	8 (42)	0.001
Diabetes mellitus	6 (13)	4 (14)	2 (10)	0.58
Prior hypertension	23 (50)	18 (67)	6 (32)	0.02
Prior hypercholesterolaemia	25 (54)	12 (44)	12 (63)	0.21
hs-CRP (mg/L)	3.5 (1.4–7.8)	2.7 (1.4–5.8)	5.6 (2.0–11.7)	0.08
Medications				
Aspirin	28 (61)	10 (37)	19 (100)	<0.001
Clopidogrel	19 (41)	4 (14)	19 (100)	<0.001
Statin	31 (67)	13 (48)	19 (100)	<0.001
β-Blocker	27 (59)	8 (30)	19 (100)	<0.001
ACEi/ARB	31 (67)	10 (37)	18 (95)	<0.001
Calcium channel blocker	7 (15)	6 (22)	1 (5)	0.11

Categorical data are displayed as n (%).
Continuous data are displayed as median (IQR).
*P values are quoted for comparisons between matched stable and unstable groups.
ACEi, ACE-inhibitor; ARB, angiotensin receptor blocker; AS, aortic stenosis; BMI, body mass index; BP, blood pressure; CAD, coronary artery disease; CVD, cerebrovascular disease; IHD, ischaemic heart disease; MI, myocardial infarction; PCI, percutaneous coronary intervention; hs-CRP, high-sensitivity C reactive protein.
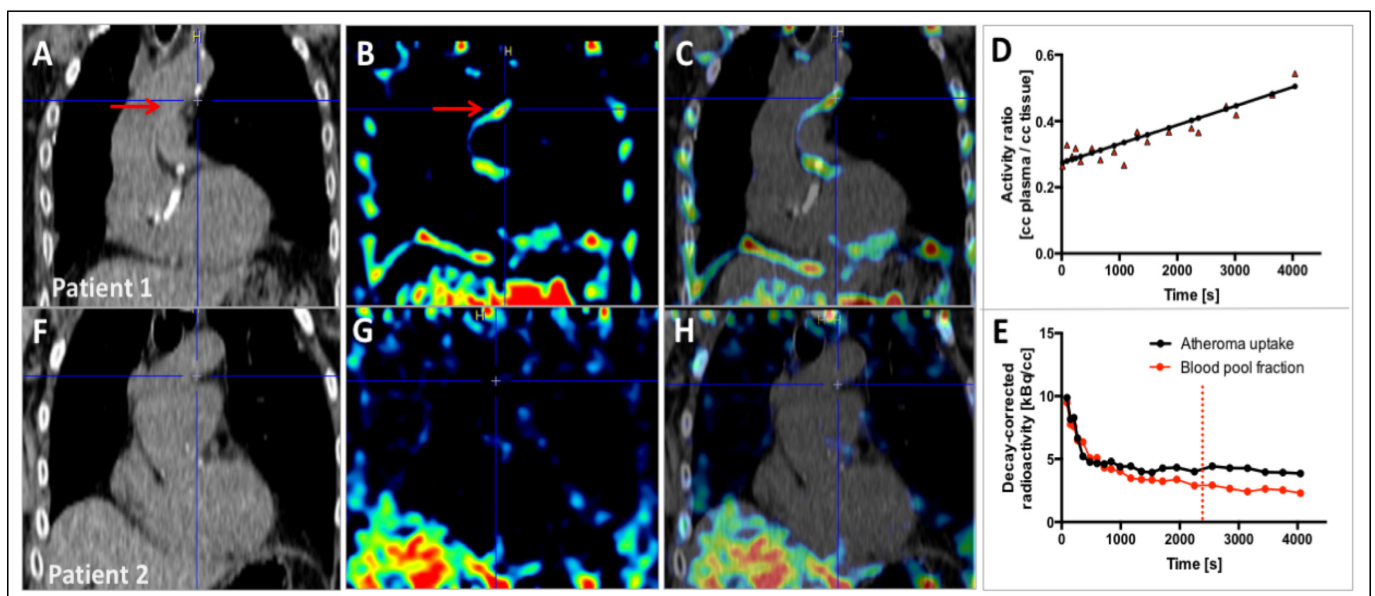
Figure 2 Kinetic analysis of aortic 18F-fluciclatide uptake. Sagittal views of the thorax following kinetic analysis in two participants with (patient 1: A–E) and without (patient 2: F–H) aortic arch 18F-fluciclatide uptake. CT images confirm presence (A) or absence (F) of aortic arch calcification as a marker of established atheroma. Patlak slope (Ki) parametric images (B and G) identify focal uptake within the aortic arch in the region of atheroma (red arrow) localising to the vessel wall on the fused Patlak and CT images (C and H). Patlak modelling (D) confirms irreversible integrin binding within the region of aortic arch calcification (red arrow). Time activity curves (TAC) within the same region (E) show a persistently high blood pool fraction, but uptake within atheroma that exceeds the blood pool fraction beyond 40 min (dashed line).

Table 2 Imaging results

	All (n=46)	Stable atherosclerosis (n=27)	Matched stable atherosclerosis (n=19)*	Unstable atherosclerosis (n=19)	P value†
18F-Fluciclatide PET uptake					
SVC (SUV_{mean})	2.73 (2.35–3.05)	2.66 (2.21–2.96)	2.47 (2.07–2.78)	2.88 (2.61–3.26)	0.01
Whole aorta (*mean SUV_{max}*)	3.65 (3.04–4.01)	3.43 (2.95–3.81)	3.04 (2.86–3.61)	3.87 (3.46–4.12)	0.002
Whole aorta (*mean TBR_{max}*)	1.31 (1.20–1.39)	1.29 (1.20–1.38)	1.25 (1.19–1.36)	1.32 (1.17–1.42)	0.32
Ascending aorta (*mean TBR_{max}*)	1.32 (1.23–1.37)	1.27 (1.23–1.36)	1.24 (1.20–1.34)	1.33 (1.18–1.39)	0.10
Aortic Arch (*mean TBR_{max}*)	1.28 (1.16–1.40)	1.27 (1.14–1.37)	1.21 (1.13–1.33)	1.29 (1.25–1.44)	0.02
Descending aorta (*mean TBR_{max}*)	1.31 (1.19–1.42)	1.30 (1.23–1.41)	1.26 (1.17–1.41)	1.32 (1.12–1.45)	0.97
CT calcium score					
Whole aorta (*AU*)	95 (0–852)	326 (11–1114)	36 (0–469)	19 (0–483)	0.85
Ascending aorta (*AU*)	0 (0–11)	0 (0–46)	0 (0–0)	0 (0–0)	0.15
Aortic arch (*AU*)	29 (0–352)	102 (0–586)	13 (0–469)	0 (0–263)	0.76
Descending aorta (*AU*)	7.5 (0–78)	0 (0–123)	0 (0–123)	8 (0–71)	0.43
CTA plaque analysis (descending aorta)					
Mean wall thickness (*% vessel diameter*)	9.1 (6.5–12.8)	8.0 (6.3–10.0)	8.1 (6.3–9.8)	12.8 (8.6–18.4)	0.009
Plaque burden (*% total volume*)	8.3 (6.1–11.4)	7.4 (6.0–9.1)	7.5 (5.9–8.9)	11.4 (7.9–15.6)	0.008

Data are presented as median (IQR).

CTA, computed tomography angiography.

* Stable group subjects paired to equivalent calcium score in unstable group.

† P values are quoted for comparisons between matched stable and unstable groups.

AU, arbitrary units; CTA, Computed Tomography Angiography; PET, positron emission tomography; SUV, standard uptake value; SVC, superior vena cava; TBR, tissue-to-background ratio.

component with a slower clearance component, causing relatively high residual blood pool activity during PET acquisition (40–70 min postinjection, SVC SUV_{mean} 2.73 (IQR 2.35–3.05); figure 2). Consequently, while 18F-fluciclatide uptake in aortic atheroma was measurable above background, TBR_{max} were relatively low (TBR_{max} range 1.08–1.68; tables 2 and 3, figures 2 and 3). In the 3-D Patlak slope (Ki) parametric images, six datasets (30%) were uninterpretable due to patient movement. In the remaining studies, increased aortic 18F-fluciclatide uptake was observed in half of subjects. Patlak modelling demonstrated a discernible linear phase suggesting irreversible ligand-receptor binding over the selected acquisition time and a greater Ki slope in these subjects compared with patients with no aortic uptake (figure 2). Subjects with uptake present on Patlak analysis (n=7)

also appeared to have higher 18F-fluciclatide uptake on standard analysis (TBR_{max} 1.32±0.05 vs 1.19±0.03, p=0.08) and greater aortic calcification (aortic calcium score 704 (28–1788) vs 0 (0–119) AU, p=0.06) than those without visible uptake, although this did not reach statistical significance.

Aortic 18F-fluciclatide uptake reproducibility studies
Using static PET images, quantification of 18F-fluciclatide blood-pool activity demonstrated excellent interobserver reproducibility, with no fixed or proportional bias (SUV_{mean} mean difference; −0.11 (−0.36–0.15)) and a good ICC coefficient (0.95, online supplementary table S2). Quantification of aortic 18F-fluciclatide uptake using the established mean TBR_{max}

Table 3 PET uptake and baseline characteristics

	Total aortic 18F-fluciclatide uptake		
	All patients	Stable cohort	Unstable cohort
Continuous variables			
CT calcium score (log10 AU)	r=0.37 (0.08–0.60), p=0.01	r=0.62 (0.43–0.81), p<0.001	r=0.20 (−0.28–0.60), p=0.41
Mean wall thickness (% vessel diameter)*	r=0.57 (0.28–0.76), p<0.001	r=0.18 (−0.26–0.56), p=0.43	r=0.69 (0.15–0.91), p=0.02
Plaque volume (% total volume)*	r=0.56 (0.26–0.75), p<0.001	r=0.16 (−0.28–0.55), p=0.47	r=0.68 (0.13–0.90), p=0.02
Log10 hs-CRP (mg/L)	r=0.18 (−0.14–0.46), p=0.28	r=0.32 (−0.07–0.62), p=0.10	r=−0.24 (−0.63–0.24), p=0.06
Categorical variables			
Hypertension (mean TBR_{max})	1.33 (1.19–1.39) vs 1.29 (1.20–1.40), p=0.91	1.27 (1.21–1.38) vs 1.33 (1.19–1.38), p=0.90	
Established ischaemic heart disease (mean TBR_{max})	1.34 (1.22–1.42) vs 1.25 (1.19–1.35), p=0.15	1.37 (1.37–1.42) vs 1.25 (1.19–1.35), p=0.04	
Hypercholesterolaemia (mean TBR_{max})	1.34 (1.21–1.42) vs 1.27 (1.19–1.34), p=0.17	1.36 (1.29–1.41) vs 1.25 (1.19–1.30), p=0.01	
Diabetes mellitus (mean TBR_{max})	1.37 (0.32–0.45) vs 1.29 (1.19–1.38), p=0.09	1.37 (1.28–1.58) vs 1.29 (1.19–1.37), p=0.15	
Current smokers (mean TBR_{max})	1.32 (1.24–1.49) vs 1.29 (1.19–1.39), p=0.54	*N* too small	

*18F-Fluciclatide uptake assessed in the descending aorta only, to correspond with CT analysis.

AU, arbitrary units; PET, positron emission tomography; TBR, tissue-to-background ratio; hs-CRP, high sensitivity C-reactive protein.
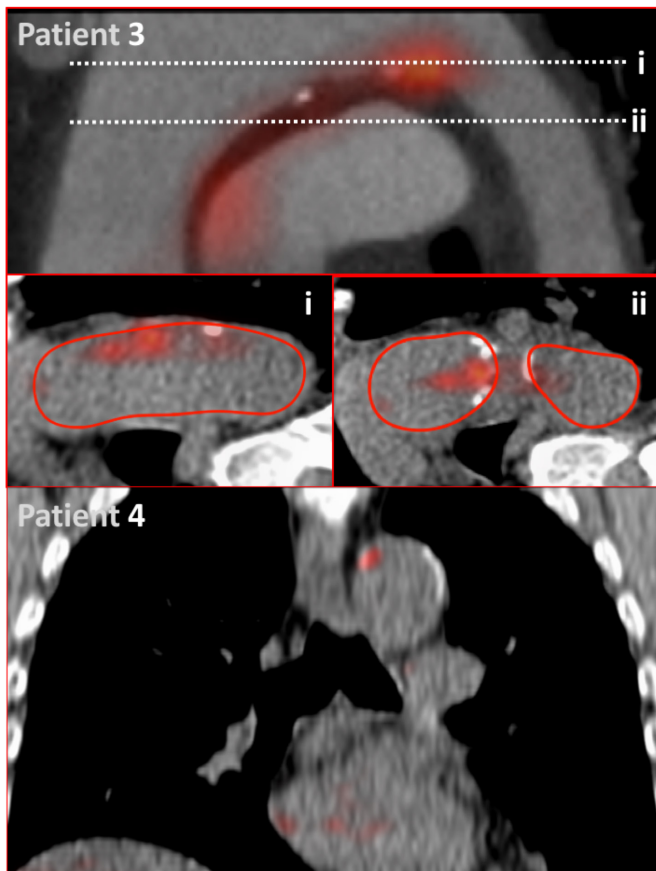
Figure 3 18F-Fluciclatide aortic uptake. Patient 3: modified coronal view of the aortic arch showing radiotracer uptake at the inner curvature of the aortic arch related to a region of aortic calcification. This activity is demonstrated on axial sections of the aorta (i and ii). Red lines indicate the adventitial borders of the aortic arch used for quantification of PET uptake. Patient 4: sagittal view of the thorax displaying focal 18F-fluciclatide uptake within a region of vascular calcification in the aortic arch.

approach[5][20] also displayed no fixed or proportional bias (mean difference; 0.08 (−0.01–0.16)) with good ICC (0.92) (online supplementary table S1).

Aortic 18F-fluciclatide uptake and atheroma burden

Our study cohort comprised patients with a wide spectrum of aortic atherosclerotic burden (aortic calcium score range 0–6857 AU). On static PET images, aortic 18F-fluciclatide uptake demonstrated a moderate relationship with disease burden in the aorta using both CT calcium scoring (r=0.37 (0.08–0.60), p=0.01) and the indexed plaque volume (r=0.56 (0.26–0.75); p<0.001) (table 3, figures 3 and 4). A good correlation was also observed with the relative vessel wall thickness (expressed as a percentage of vessel diameter, r=0.57 (0.28–0.76); p<0.001). There was no correlation between aortic 18F-fluciclatide uptake and the inflammatory marker CRP ($\log_{10}$ hs-CRP r=0.18, p=0.28).

Aortic 18F-fluciclatide uptake in stable and unstable patients

To establish whether 18F-fluciclatide uptake may be a marker of unstable atherosclerotic activity, we compared aortic uptake in patients who had sustained a recent MI with those in our stable cohort. Given the association demonstrated between 18F-fluciclatide activity and plaque burden, we matched patients in the two groups according to CT calcium score (online
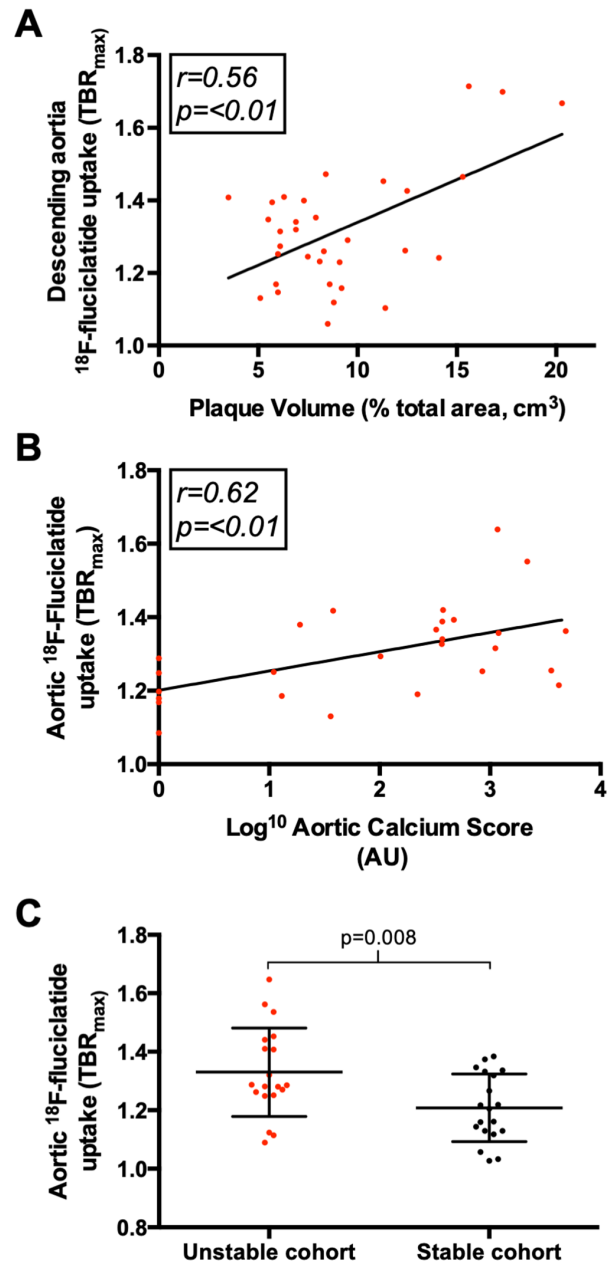
Figure 4 18F-Fluciclatide uptake, atheroma burden and clinical stability. Graphs displaying the relationship between aortic 18F-fluciclatide uptake and aortic plaque burden, assessed using both the plaque volume (A) and calcium score (B). Moreover, 18F-fluciclatide uptake was greater in patients with *unstable* (recent myocardial infarction) vs *stable* (no recent cardiovascular events) atherosclerotic disease (C). TBR, tissue-to-background ratio.

supplementary table S2). We demonstrated increased 18F-fluciclatide aortic arch uptake in patients with recent MI compared with those in the stable cohort (TBR_{max}; 1.29 (IQR 1.25–1.44) vs 1.20 (1.13–1.33, p=0.02)) despite equivalent aortic calcium scores (table 2, figure 4). Moreover, in patients with recent MI, a stronger correlation was observed between aortic plaque burden and 18F-fluciclatide uptake than in the patient population as a whole (aortic wall thickness r=0.68, p=0.02). When aortic SUV measurement were assessed, these were consistently increased in the unstable groups compared with the stable groups across all regions of the aorta, even before attempts were made to match

these groups by calcium score (p<0.05 for all aortic regions, table 2 and online supplementary table S3).

Aortic 18F-fluciclatide and cardiovascular risk factors

Among patients in the stable cohort, aortic 18F-fluciclatide uptake correlated with a number of risk factors (table 3). 18F-Fluciclatide activity was higher in patients with hypercholesterolaemia compared with those without (TBR$_{max}$; 1.36 (IQR 1.29–1.41) vs 1.25 (IQR 1.19–1.30), p=0.01) and those with a diagnosis of coronary heart disease (TBR$_{max}$; 1.37 (IQR 1.37–1.42) vs 1.25 (IQR 1.19–1.35), p=0.04) . An apparent observed trend was also seen in patients with diabetes (TBR$_{max}$; 1.37 (1.28–1.58) vs 1.29 (1.19–1.37), p=0.15), although this did not meet statistical significance. Again, a strong correlation was observed between 18F-fluciclatide uptake and the CT calcium score (r=0.62, p<0.001) in this subgroup.

DISCUSSION

We present the largest multimodality imaging study to date evaluating the application of an RGD-based $\alpha_v\beta_3$ integrin receptor radiotracer in the assessment of human atheroma. We have demonstrated that ex vivo 18F-fluciclatide binding co-localises to sites of $\alpha_v\beta_3$ integrin receptor expression in excised carotid plaques, and this was associated with regions of both angiogenesis and inflammation. We have further demonstrated in vivo that 18F-fluciclatide uptake increased with progressive atherosclerotic plaque burden and is higher in patients with unstable versus stable atherosclerotic disease. These data would suggest that 18F-fluciclatide holds promise as a non-invasive marker of disease activity in atherosclerosis, informing us about two key characteristics of high-risk atheroma: inflammation and angiogenesis. RGD-based tracers may therefore aid our pathophysiological understanding of this important condition and help identify patients at increased risk of adverse cardiovascular events.

Plaque inflammation and angiogenesis are two key pathological processes associated with atheroma progression, plaque rupture and clinical events. Macrophages drive expansion of the necrotic core and secrete matrix metalloproteinases that weaken the fibrous cap, predisposing it to rupture. Angiogenesis is believed to occur in response to hypoxic conditions within the necrotic core and is associated with high-risk plaque characteristics.[3] In addition, these new vessels are prone to leakage and rupture resulting in plaque haemorrhage that itself results in a pro-inflammatory response, plaque destabilisation and clinical events. A non-invasive imaging technique that can inform about the activity of these two adverse pathological processes might therefore be useful in identifying patients with active high-risk atheroma. Indeed, it is hoped that non-invasive markers of systemic atherosclerotic disease activity may identify the vulnerable patient and provide incremental risk prediction to an assessment of radiographic coronary or carotid disease burden alone.[2 23] We have here demonstrated that 18F-fluciclatide PET-CT is an emerging and promising approach to achieve these aims.

Our autoradiographic data showed focal 18F-fluciclatide binding within carotid atheroma that localised histologically to $\alpha_v\beta_3$ integrin expression with no evidence of non-specific binding. Regions of 18F-fluciclatide uptake on autoradiography also corresponded to sites of immunohistochemical cellular staining for vascular endothelial cells and macrophages. This is in keeping with previous RGD-radiotracer studies and supports its role as a selective marker for angiogenic and inflammatory components of atherosclerotic activity.[7 24 25] Due to the close relationship between intraplaque inflammation and angiogenesis

however, we are unable to ascertain whether 18F-fluciclatide was binding preferentially to one or the other of these processes.

Dynamic in vivo imaging studies in 20 subjects confirmed irreversible 18F-fluciclatide binding to regions of aortic atherosclerosis over the selected acquisition time, and demonstrated that the optimum time for 18F-fluciclatide imaging in the aorta is between 40 and 70 min. This timeframe was used for subsequent static PET imaging across the cohort as a whole. Static in vivo imaging demonstrated reproducible quantification of 18F-fluciclatide in aortic atheroma of all 46 patients, and this was correlated with the severity of aortic atherosclerotic burden, itself a manifestation of systemic atherosclerosis and a strong predictor of cardiovascular events.[26 27] Indeed, associations were observed with the aortic calcium score, aortic wall thickness and overall plaque volume. In patients with clinically stable disease, aortic uptake of 18F-fluciclatide was increased in subjects with hypercholesterolaemia and those with ischaemic heart disease, with a trend towards higher uptake in patients with diabetes mellitus that did not meet statistical significance. Perhaps most importantly, 18F-fluciclatide uptake in aortic atheroma was increased in patients with unstable (recent MI) versus stable clinical disease. Interestingly, using 18F-fluorodeoxyglucose, we have previously demonstrated a similar pattern of increased metabolic activity in aortic atheroma among patients with recent MI.[28] These data therefore lend support to the hypothesis that acute MI causes inflammation and instability in systemic atherosclerosis, as has been suggested in preclinical murine models.[29] It also provides further validity to the concept that 18F-fluciclatide uptake can identify higher risk plaques. However, whether this increased disease activity truly represents a response to the infarct or rather the underlying trigger remains to be determined.

We acknowledge that there are limitations of our study that include potential partial volume artefacts, a limited histological assessment and the use of surrogate measures for aortic histology. 18F-Fluciclatide imaging prior to carotid endarterectomy would allow for a more direct comparison between in vivo imaging and histological assessment and consolidate our findings in line with previous publications.[7] Furthermore, our exploratory assessment of aortic plaque volume may not take into account non-atheromatous intimal thickening in response to chronic hypertension. The dynamic imaging approach proved sensitive to patient movement during the prolonged acquisition period, limiting its utility in quantitative analysis, but this may ultimately be readdressed by novel motion tracking systems that allow for correction of cardiac and respiratory motion, enabling even greater definition of regional $\alpha_v\beta_3$ integrin expression.[30] Furthermore, given the limited number of patients studied using univariate analyses, we cannot exclude confounding of our results by other factors, nor that due to the multiple comparisons made, some tests may be statistically significant by chance alone. Nonetheless, we believe that the totality of our comprehensive evidence using multiple approaches and imaging modalities provides a robust and cogent argument to support our findings.

In conclusion, this is the largest study to date assessing $\alpha_v\beta_3$ integrin expression in human atherosclerotic disease. We have demonstrated that 18F-fluciclatide uptake localises to regions of inflammation and angiogenesis, correlates with the plaque burden and is increased in patients with clinically unstable disease. Although further study is required, our data indicate that 18F-fluciclatide shows promise as a non-invasive marker of disease activity and instability in atherosclerosis.

Key messages

What is already known on this subject?
► The alpha-V beta-3 ($\alpha_v\beta_3$) integrin receptor is a mediator of plaque angiogenesis and inflammation and has been targeted as a potential marker of atherosclerotic activity using positron emission tomography radiotracers.
► Studies of $\alpha_v\beta_3$ integrin-specific radiotracers in humans are lacking.

What might this study add?
► This is the largest study to date assessing $\alpha_v\beta_3$ integrin expression in human atherosclerosis.
► We have demonstrated that 18F-fluciclatide uptake localises to vascular inflammation and angiogenesis, correlates with plaque burden and is increased in patients with clinically unstable disease.

How might this impact on clinical practice?
► Non-invasive markers of atherosclerotic disease activity may identify vulnerable patients and provide incremental risk prediction to current anatomic imaging approaches.
► In this study, 18F-fluciclatide shows promise as a non-invasive marker of disease activity and instability in atherosclerosis.

ORCID iDs
William S Jenkins http://orcid.org/0000-0001-8872-0413
James HF Rudd http://orcid.org/0000-0003-2243-3117

REFERENCES
1 Mozaffarian D, Benjamin EJ, Go AS, et al. Heart disease and stroke statistics—2015 update. *Circulation* 2015;131:e29–322.
2 Dweck MR, Aikawa E, Newby DE, et al. Noninvasive molecular imaging of disease activity in atherosclerosis. *Circ Res* 2016;119:330–40.
3 Dweck MR, Doris MK, Motwani M, et al. Imaging of coronary atherosclerosis - evolution towards new treatment strategies. *Nat Rev Cardiol* 2016;13:533–48.
4 Rudd JHF, Myers KS, Bansilal S, et al. 18Fluorodeoxyglucose positron emission tomography imaging of atherosclerotic plaque inflammation is highly reproducible. *J Am Coll Cardiol* 2007;50:892–6.
5 Joshi NV, Vesey AT, Williams MC, et al. 18F-fluoride positron emission tomography for identification of ruptured and high-risk coronary atherosclerotic plaques: a prospective clinical trial. *Lancet* 2014;383:705–13.
6 Dweck MR, Chow MWL, Joshi NV, et al. Coronary arterial 18F-Sodium fluoride uptake. *J Am Coll Cardiol* 2012;59:1539–48.
7 Beer AJ, Pelisek J, Heider P, et al. Pet/Ct imaging of integrin αvβ3 expression in human carotid atherosclerosis. *JACC Cardiovasc Imaging* 2014;7:178–87.
8 ten Kate GL, Sijbrands EJG, Valkema R, et al. Molecular imaging of inflammation and intraplaque vasa vasorum: a step forward to identification of vulnerable plaques? *J Nucl Cardiol* 2010;17:897–912.
9 Mena E, Owenius R, Turkbey B, et al. [18F]fluciclatide in the in vivo evaluation of human melanoma and renal tumors expressing αvβ 3 and α vβ 5 integrins. *Eur J Nucl Med Mol Imaging* 2014;41:1879–88.
10 Kenny LM, Coombes RC, Oulie I, et al. Phase I trial of the positron-emitting Arg-Gly-Asp (RGD) peptide radioligand 18F-AH111585 in breast cancer patients. *J Nucl Med* 2008;49:879–86.
11 Yoo JS, Lee J, Jung JH, et al. SPECT/CT imaging of high-risk atherosclerotic plaques using integrin-binding RGD dimer peptides. *Sci Rep* 2015;5:11752.
12 Su H, Gorodny N, Gomez LF, et al. Atherosclerotic plaque uptake of a novel integrin tracer 18F-Flotegatide in a mouse model of atherosclerosis. *J Nucl Cardiol* 2014;21:553–62.
13 Vancraeynest D, Roelants V, Bouzin C, et al. αVβ3 integrin-targeted microSPECT/CT imaging of inflamed atherosclerotic plaques in mice. *EJNMMI Res* 2016;6:29.
14 Laitinen I, Saraste A, Weidl E, et al. Evaluation of alphavbeta3 integrin-targeted positron emission tomography tracer 18F-galacto-RGD for imaging of vascular inflammation in atherosclerotic mice. *Circ Cardiovasc Imaging* 2009;2:331–8.
15 Tomasi G, Kenny L, Mauri F, et al. Quantification of receptor-ligand binding with [18F]fluciclatide in metastatic breast cancer patients. *Eur J Nucl Med Mol Imaging* 2011;38:2186–97.
16 McParland BJ, Miller MP, Spinks TJ, et al. The biodistribution and radiation dosimetry of the Arg-Gly-Asp peptide 18F-AH111585 in healthy volunteers. *J Nucl Med* 2008;49:1664–7.
17 Jenkins WSA, Vesey AT, Stirrat C, et al. Cardiac $\alpha_v\beta_3$ integrin expression following acute myocardial infarction in humans. *Heart* 2017;103:607–15.
18 Dweck MR, Jenkins WSA, Vesey AT, et al. 18F-sodium fluoride uptake is a marker of active calcification and disease progression in patients with aortic stenosis. *Circ Cardiovasc Imaging* 2014;7:371-8.
19 Niccoli Asabella A, Ciccone MM, Cortese F, et al. Higher reliability of 18F-FDG target background ratio compared to standardized uptake value in vulnerable carotid plaque detection: a pilot study. *Ann Nucl Med* 2014;28:571–9.
20 Dweck MR, Jones C, Joshi NV, et al. Assessment of valvular calcification and inflammation by positron emission tomography in patients with aortic stenosis. *Circulation* 2012;125:76–86.
21 Dweck MR, Khaw HJ, Sng GKZ, et al. Aortic stenosis, atherosclerosis, and skeletal bone: is there a common link with calcification and inflammation? *Eur Heart J* 2013;34:1567–74.
22 Bland JM, Altman DG. Statistical methods for assessing agreement between two methods of clinical measurement. *Lancet* 1986;1:307–10.
23 Arbab-Zadeh A, Fuster V. The myth of the 'vulnerable plaque': transitioning from a focus on individual lesions to atherosclerotic disease burden for coronary artery disease risk assessment. *J Am Coll Cardiol* 2015;65:846–55.
24 Golestani R, Mirfeizi L, Zeebregts CJ, et al. Feasibility of [18F]-RGD for ex vivo imaging of atherosclerosis in detection of αvβ3 integrin expression. *J Nucl Cardiol* 2015;22:1179–86.
25 Sun Y, Zeng Y, Zhu Y, et al. Application of (68)Ga-PRGD2 PET/CT for αvβ3-integrin imaging of myocardial infarction and stroke. *Theranostics* 2014;4:778–86.
26 Hong SN, Gona P, Fontes JD, et al. Atherosclerotic biomarkers and aortic atherosclerosis by cardiovascular magnetic resonance imaging in the Framingham heart study. *J Am Heart Assoc* 2013;2.
27 Dutta P, Courties G, Wei Y. Aortic calcified plaques and cardiovascular disease (the Framingham study) 2004:1–5.
28 Joshi NV, Toor I, Shah ASV, et al. Systemic atherosclerotic inflammation following acute myocardial infarction: myocardial infarction begets myocardial infarction. *J Am Heart Assoc* 2015;4:e001956.
29 Dutta P, Courties G, Wei Y, et al. Myocardial infarction accelerates atherosclerosis. *Nature* 2012;487:325–9.
30 Rubeaux M, Joshi NV, Dweck MR, et al. Motion correction of 18F-NaF PET for imaging coronary atherosclerotic plaques. *J Nucl Med* 2016;57:54–9.